BRL
2714
C.1A

NOV 1986
CIRCULATING COPY

AD A167046

TECHNICAL REPORT BRL-TR-2714

CAVITY COLLAPSE IGNITION OF COMPOSITION B IN THE LAUNCH ENVIRONMENT

John J. Starkenberg
Doenee L. McFadden
Ona R. Lyman

February 1986

APPROVED FOR PUBLIC RELEASE; DISTRIBUTION UNLIMITED.

US ARMY BALLISTIC RESEARCH LABORATORY
ABERDEEN PROVING GROUND, MARYLAND

Destroy this report when it is no longer needed.
Do not return it to the originator.

Additional copies of this report may be obtained from the National Technical Information Service, U. S. Department of Commerce, Springfield, Virginia 22161.

The findings in this report are not to be construed as an official Department of the Army position, unless so designated by other authorized documents.

The use of trade names or manufacturers' names in this report does not constitute indorsement of any commercial product.

UNCLASSIFIED

SECURITY CLASSIFICATION OF THIS PAGE (When Data Entered)

REPORT DOCUMENTATION PAGE		READ INSTRUCTIONS BEFORE COMPLETING FORM
1. REPORT NUMBER **Technical Report BRL-TR-2714**	2. GOVT ACCESSION NO.	3. RECIPIENT'S CATALOG NUMBER
4. TITLE (and Subtitle) Cavity Collapse Ignition of Composition B in the Launch Environment		5. TYPE OF REPORT & PERIOD COVERED 6. PERFORMING ORG. REPORT NUMBER
7. AUTHOR(s) John Starkenberg Doenee L. McFadden Ona R. Lyman		8. CONTRACT OR GRANT NUMBER(s)
9. PERFORMING ORGANIZATION NAME AND ADDRESS **U.S. Army Ballistic Research Laboratory** ATTN: SLCBR-TB Aberdeen Proving Ground, MD. 21005-5066		10. PROGRAM ELEMENT, PROJECT, TASK AREA & WORK UNIT NUMBERS 1L161102AH43
11. CONTROLLING OFFICE NAME AND ADDRESS **U.S. Army Ballistic Research Laboratory** ATTN: **SLCBR-DD-T** Aberdeen Proving Ground, MD. 21005-5066		12. REPORT DATE **February 1986** 13. NUMBER OF PAGES **36**
14. MONITORING AGENCY NAME & ADDRESS (if different from Controlling Office)		15. SECURITY CLASS. (of this report) 15a. DECLASSIFICATION/DOWNGRADING SCHEDULE

16. DISTRIBUTION STATEMENT (of this Report)

Approved for public release, distribution unlimited.

17. DISTRIBUTION STATEMENT (of the abstract entered in Block 20, if different from Report)

18. SUPPLEMENTARY NOTES

19. KEY WORDS (Continue on reverse side if necessary and identify by block number)

Explosive sensitivity, setback, prematures, adiabatic compression, compressive heating, deformation heating.

20. ABSTRACT (Continue on reverse side if necessary and identify by block number)

Experiments using the activator at the Ballistic Research Laboratory have been pursued for a number of years with an eye toward clarifying the mechanisms involved in the premature ignition of high explosives in the setback environment. Recently, we have turned our attention to a series of experiments in which controlled cavities in cast Composition B are subjected to deformation both with and without simultaneous air compression as well as air compression without deformation. The dimple tests were designed to accomplish this. There are three variations of the dimple test. In the

DD FORM 1 JAN 73 1473 EDITION OF 1 NOV 65 IS OBSOLETE

UNCLASSIFIED

SECURITY CLASSIFICATION OF THIS PAGE (When Data Entered)

standard dimple test a cylindrical cavity or dimple of controlled depth and diameter is cast into one end of the explosive sample. In another variation, vacuum hardware is used. In a third variation, the dimple is cast into a piece of Dow Corning Sylgard 182 which is placed in contact with an undimpled explosive sample. In the vacuum dimple test, only deformation heating can produce an ignition. In the Sylgard dimple test, only air compression heating occurs. Both heating mechanisms are combined in the standard dimple test. To date, only Composition B has been subjected to dimple testing. As a result of our work thus far, we have found that when the air compression and deformation heating mechanisms are combined the dominant ignition mechanism is compressive heating of air strongly influenced by the cavity collapse geometry and possibly by alteration of the state of the explosive surface. The hypothesis of a transition from axial to radial cavity collapse with increasing dimple depth seems to explain the observed behavior. Deformation heating is the dominant mechanism only for high aspect ratio dimples.

TABLE OF CONTENTS

This page Left Intentionally Blank

LIST OF ILLUSTRATIONS

This page Left Intentionally Blank

I. INTRODUCTION

Experiments using the activator at the Ballistic Research Laboratory (BRL) have been pursued for a number of years with an eye toward clarifying the mechanisms involved in the premature ignition of high explosives in the setback environment.[1-4] In a broader sense, however, this research sheds light on the very minimum stimulus levels which cause violent reaction in explosives and may be pertinent to ignition in a variety of circumstances.

The relationship of laboratory scale experiments and large scale "simulation", such as with the Naval Surface Weapons Center (NSWC) simulator[5-7] to gun firings is a difficult issue. The appropriate role of **laboratory experiments is not the simulation of the artillery launch** environment, but rather the study of ignition mechanisms under pressures representative of setback. The experiments reported herein were conducted in this spirit. Therefore, the activator experimental procedure is not (as it has been called) "an increased severity test." Rather, it is an isolated stimulus experiment which is designed to determine the level of air compression heating or other stimulus required to ignite an explosive as a function of various parameters. If a premature occurred due to compressive heating ignition, we would conclude that the explosive was locally subjected to the same stimulus level determined in our experiments. In general, this means that the explosive must be subject to the same heating rate. In the case of compressive heating, the heating rate is roughly proportional to the product of the pressurization rate and the cavity depth. In the case of frictional or shear heating, the heating rate is roughly proportional to the product of the pressure and the shear velocity. In both cases, many other factors are also important. Pressurization rates and peak pressures measured external to projectile bases appear insufficient to produce the required stimulus. The maximum sliding velocity produced by projectile rotation is somewhat below that required for ignition observed in activator experiments isolating frictional heating.[8] This means that, in order to produce a premature, the stimulus levels applied to the explosive must be amplified over and above those present external to the projectile during launch. This may occur in a number of ways. In the case of compressive heating, one way is to amplify the pressurization rate. This can occur if a loose charge impacts the base or if a cavity fails to collapse during the early portion of pressurization and then collapses catastrophically when a critical pressure has been reached. A cavity collapse geometry which concentrates heated air on a small portion of the explosive surface also amplifies the stimulus level. In addition, as a cavity **collapses, shear heating may combine with compressive heating to produce an** ignition. Hershkowitz[9] has suggested that prematures are rare because they require two or more low probability conditions to exist simultaneously. For example, a sufficiently large cavity must be coupled with an abnormally severe launch environment. The relationship between the local heating rate experienced by an explosive fill and the pressure stimulus external to the projectile is complicated and has not been established. We have not pursued this avenue. Our approach has been to determine the parameters which govern ignition by the most likely mechanisms in order to provide guidance for the design of more premature-resistant projectile systems.

II. REVIEW OF COMPRESSIVE HEATING OBSERVATIONS

When a small volume of gas is compressed very rapidly such that no energy transport can occur, a high temperature reservoir (hot spot) is created which may subsequently heat an adjacent explosive layer to the point of ignition. This process is referred to as ignition by adiabatic compression of the gas. If, on the other hand, the gas is compressed very slowly, no temperature increase occurs and no explosive ignition can follow. Between these limits lies the compressive heating regime in which the compression occurs sufficiently slowly that considerable energy is transported by conduction and convection during the process. Compressive heating has, therefore, received attention primarily as a source of ignition which is active when the observed time to ignition is in the ten microsecond to ten millisecond range, a time scale which is typical of the setback of the explosive fill in a projectile during launch.

Compressive heating ignition has been the subject of extensive analytical and experimental study at BRL. The experimental investigation was conducted using an apparatus, referred to as the activator, which was originally designed at Picatinny Arsenal as a laboratory-scale artillery setback simulator.[10] This was used in its original form in preliminary experiments to produce data which revealed the role of air in causing ignitions during compression. Subsequently, the activator was modified and further instrumented so that more definitive data could be extracted from the tests and direct comparisons to the predictions obtained from analytical models could be made. In particular, the activator has been used to explore ignition of Composition B and TNT as well as a number of other explosives caused by the rapid compression of air trapped in contact with the explosive.

A number of observations from our study of air compression heating are pertinent to the present study. As a result of our earlier testing, we learned that this is indeed a viable mechanism for ignition at relatively mild stimulus levels and we established pressurization rate and cavity size as the principal governing parameters. We found that sensitivity is substantially influenced by the geometry of cavity collapse and the state of the explosive surface. Convergent geometries, which concentrate heated air on a small portion of the explosive surface, are more sensitive as are nonporous surfaces, which prevent leakage of air away from the ignition site.

In this earlier work, care was taken to decouple the stimulus level from the explosive mechanical properties by using cavities external to the explosive which collapse without mechanical failure of the explosive. More recently, we have turned our attention to a series of experiments in which controlled cavities in cast Composition B are subjected to deformation both with and without simultaneous air compression as well as air compression without deformation. This series of tests can be used to explore the role of explosive deformation in ignition. In particular, we were interested in determining whether deformation produces sufficient heating to cause ignition or simply acts to increase the local air pressurization rate.

III. DESCRIPTION OF THE EXPERIMENTS

A. The Activator

The activator, as presently used, is illustrated schematically in Figure 1. The test section consists of a mild steel heavy confinement cylinder enclosing the explosive sample and a hardened steel driving piston. A hardened steel gage block, on which a manganin foil pressure gage is mounted, is tightly bolted to the back of the confinement cylinder and the explosive sample is inserted into the bore adjacent to the gage. A gap or cavity of some type is left adjacent to the sample. The gage block rests against a rigid stop which incorporates an adjustment screw to accommodate test fixtures of different lengths and to allow easy installation. The driving piston is activated by a larger piston which is initially held in place using shear pins. The large piston is set in motion by pressure developed in the breech which is instrumented with a pressure transducer. The free run allowed between the large piston and the driving piston is used to set the stimulus level to be applied.

In order to fire a shot, the breech is pressurized using compressed air until the shear pins fail. The large piston accelerates through the free run and impacts the driving piston. The momentum developed by the pistons is transformed to an impulse delivered to the air gap and explosive sample. The pistons may then rebound and strike the explosive again delivering a second impulse. The breech pressure begins at the shear pin failure pressure and drops linearly with time during the test to a value associated with the final volume of the breech. An average value of breech pressure during piston motion may be used in conjunction with free run to estimate the momentum of the large piston when it impacts the driving piston.

A disadvantage of this test configuration is that extrusion of explosive between the gage block and the confinement cylinder may occur. Ignitions caused by extrusion are readily identifiable as late events on the pressure records. We determined that free runs in excess of 25 mm are required to produce extrusion ignitions. This free run, therefore, represents a practical upper limit of activator operation. However, this limit was sometimes violated since it is possible to distinguish extrusion ignitions.

B. Dimple Tests

Previously, care was taken to isolate the effects of air compression from those of explosive deformation during cavity collapse. This was accomplished by placing the cavity in a material external to the explosive. The next logical step in the investigation was to develop a series of experiments in which the deformation effects are included, in isolation from as well as in combination with compressive heating. The dimple tests were designed to accomplish this.

There are three variations of the dimple test. The experimental configuration for each is shown schematically in Figure 2. In the standard dimple test, a cylindrical cavity or dimple of controlled depth and diameter is cast into one end of the explosive sample. The sample is inserted, dimple up, into the confinement cylinder. A thin polyethylene film attached to the face of the driving piston improves the seal against the face of the explosive

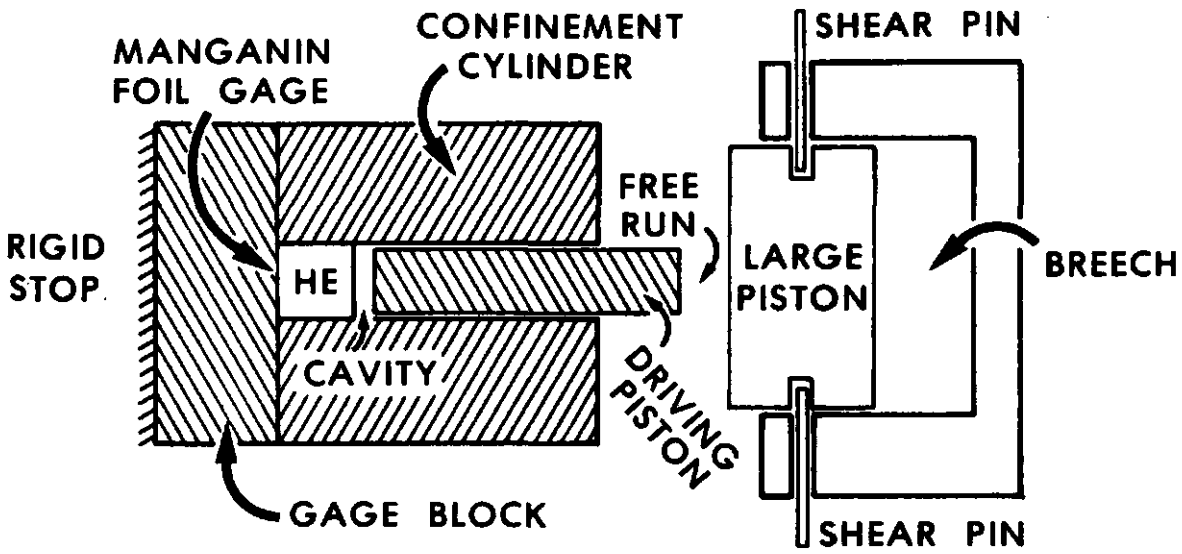

Figure 1. Activator Schematic.

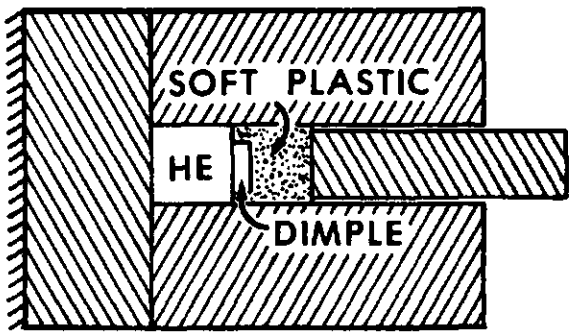

AIR COMPRESSION ONLY

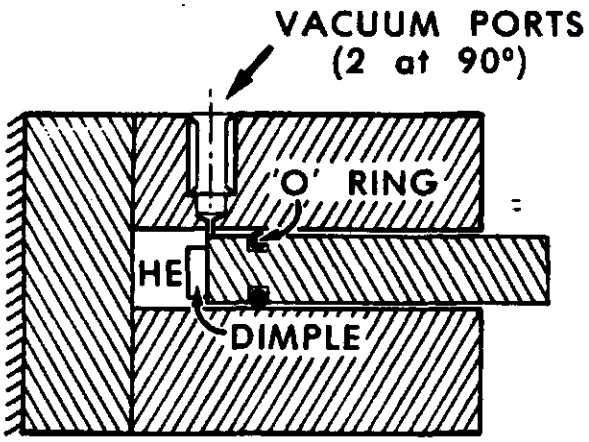

DEFORMATION ONLY

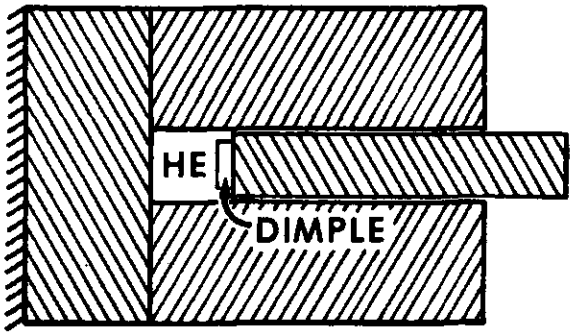

COMBINED MECHANISMS

Figure 2. Dimple Test Series.

sample. In another variation, vacuum hardware is used. Prior to firing, the piston is inserted into the bore hole but held away from the sample until sufficient vacuum has been produced using a vacuum pump. The piston is then allowed to move forward against the sample, sealing a vacuum into the dimple. The vacuum pump continues to operate until after the firing is completed. In a third variation, the dimple is cast into a piece of Dow Corning Sylgard 182 which is placed in contact with an undimpled explosive sample. All other test procedures are as previously described.

In the vacuum dimple test, only deformation heating can produce an ignition. In the Sylgard dimple test, only air compression heating occurs. Both heating mechanisms are combined in the standard dimple test.

C. Sample Preparation

The Compostion B samples were prepared by casting short 12.7-mm diameter cylinders. In order to prepare dimpled samples, a casting plate with cylindrical protrusions of adjustable height was used beneath the mold. Two different nominal dimple diameters were produced. Dimple depth and diameter were measured. For undimpled samples, a polished casting plate was used. All samples were then finished to a length of 12.7 mm by cutting and polishing the opposite end. Dimpled and undimpled samples as well as Sylgard dimples are shown in Figure 3. The densities of all samples were determined and all samples were inspected radiographically. Any sample appearing to have voids was rejected. Dimple depth and diameter were measured.

D. Characterization of Stimulus Levels

In our earlier tests with cavities external to the explosive, pressure conditions in the vicinity of the cavity could be inferred from the pressure records from the manganin gage at the base of the sample. This provided us with a pertinent characterization of the stimulus level. In the dimple test, however, the conditions as the cavity collapses are complicated and the heating rate bears no simple relation to the pressure record. The best measure of applied stimulus level must be judged, therefore, by the degree to which it segregates go and no go results in a plot of stimulus level versus cavity size.

Several pertinent measures of stimulus level are available. The simplest of these is the free run of the activator. The stimulus generally increases with increasing free run. Since the breech pressure at which the shear pins fail varies from shot to shot, the impact momentum may be calculated from the free run and the shear pin failure pressure, providing a second measure of stimulus level which should be an improvement over the free run. Note that friction is ignored. Finally, information from the manganin gage record can be used. Since this is closest to the event, it should provide the best characterization of the stimulus level. In this case, the problem of what aspect of the pressure record to use arises. Peak pressure cannot be used since the occurrence of an ignition before peak pressure is achieved obscures this information. Experience has taught us that pressurization rate is a good indicator of stimulus level. However pressurization rate is observed to vary during the test, exhibiting several peaks of approximately the same value. Either the average of the peak pressurization rates or an overall average pressurization rate which includes the plateaus or falling regions can be used.

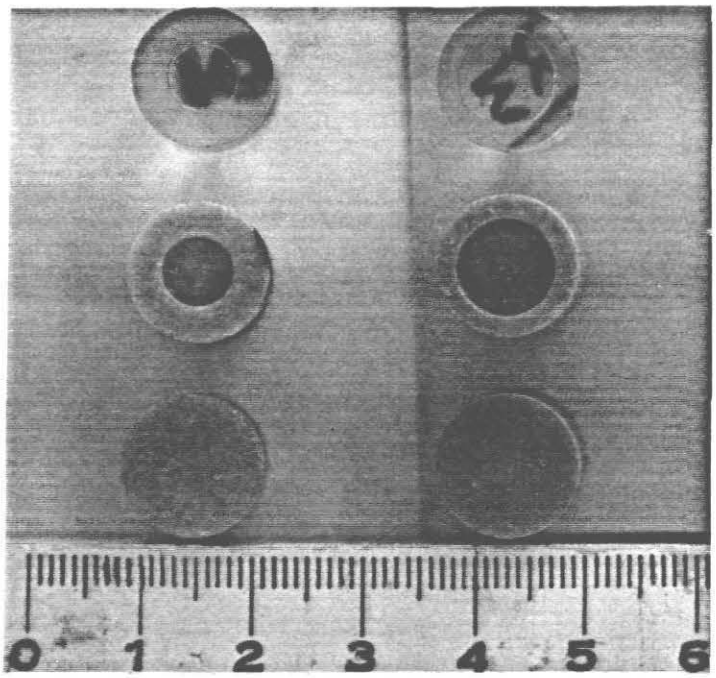

Figure 3. Dimpled and Undimpled Composition B Samples and Sylgard Dimples.

These four stimulus characterization parameters are compared in Figures 4, 5 and 6 for the three tests of the dimple series. In Figure 4, each parameter has been plotted against dimple depth for the Sylgard dimple test with Composition B. Reasonable results are achieved using free run, but impact momentum, average peak pressurization rate and average pressurization rate do not provide adequate segregation. Similar plots for the vacuum dimple test are shown in Figure 5. In this case free run is clearly best and average and average peak pressurization rates are also acceptable while impact momentum fails. Finally, the plots for standard dimples are shown in Figure 6. The best data segregation is achieved using free run. Reasonable results are also obtained with pressurization rate but a few anomalous points appear. Use of impact momentum or average pressurization rate produces a wide band of mixed data. Thus, free run is the only parameter producing good data segregation in all three tests.

IV. DIMPLE TEST RESULTS

A. General Observations

Typical manganin gage pressure records from the base of the sample are illustrated in Figure 7. The pressure histories observed may be generally categorized according to the nature of the rising portion of the impulse. When Sylgard dimples were used the pressure was observed to rise in a series of steps as in Figure 7a. The pressurization rate between the plateaus was roughly the same. Results obtained with dimpled explosives were often similar. However, the pressure was frequently observed to rise and fall quite markedly during pressurization as in Figure 7b. This occurred for both ignitions and nonignitions and is probably associated with cavity collapse.

Ignition may occur during the rising portion of the pressure history or be delayed until after the pressure has peaked. The latter behavior is more frequently observed with dimpled explosive. Samples that were recovered after firing always showed the dimple to be completely closed. Samples before and after testing are compared in the photograph of Figure 8.

B. Preliminary Observations with Composition B - Effects of Dimple Depth

To date only Composition B has been subjected to dimple testing. Nominal dimple depths of 0.4, 0.8, 1.1 and 1.5 mm with a diameter of about 8.5 mm were used in the initial test series. The plots of Figures 4a, 5a and 6a in the free run - dimple depth plane, using different symbols for ignition and nonignition, are useful for comparing the results. The results for the Sylgard dimple test are shown in Figure 4a. In this case, we observe sensitivity which increases with increasing dimple depth. This is consistant with our previous observations and is not surprising. The results of the vacuum dimple test, shown in Figure 5a, are also as expected. Ignition under vacuum was only possible with the deepest dimples at the longest free runs. The results when the mechanisms are combined in the standard dimple test are more complicated as shown in Figure 6a. No ignitions were observed with the shallowest dimples (~ 0.4 mm). Sensitivity to ignition with dimples with a nominal 0.7-mm depth exhibits a strong dependence on dimple depth. Dimples shallower than about 0.7 mm do not produce ignition while dimples slightly deeper than that produce ignition over a relatively wide range of free run. This dimple depth represents a cut-off value below which ignition does not

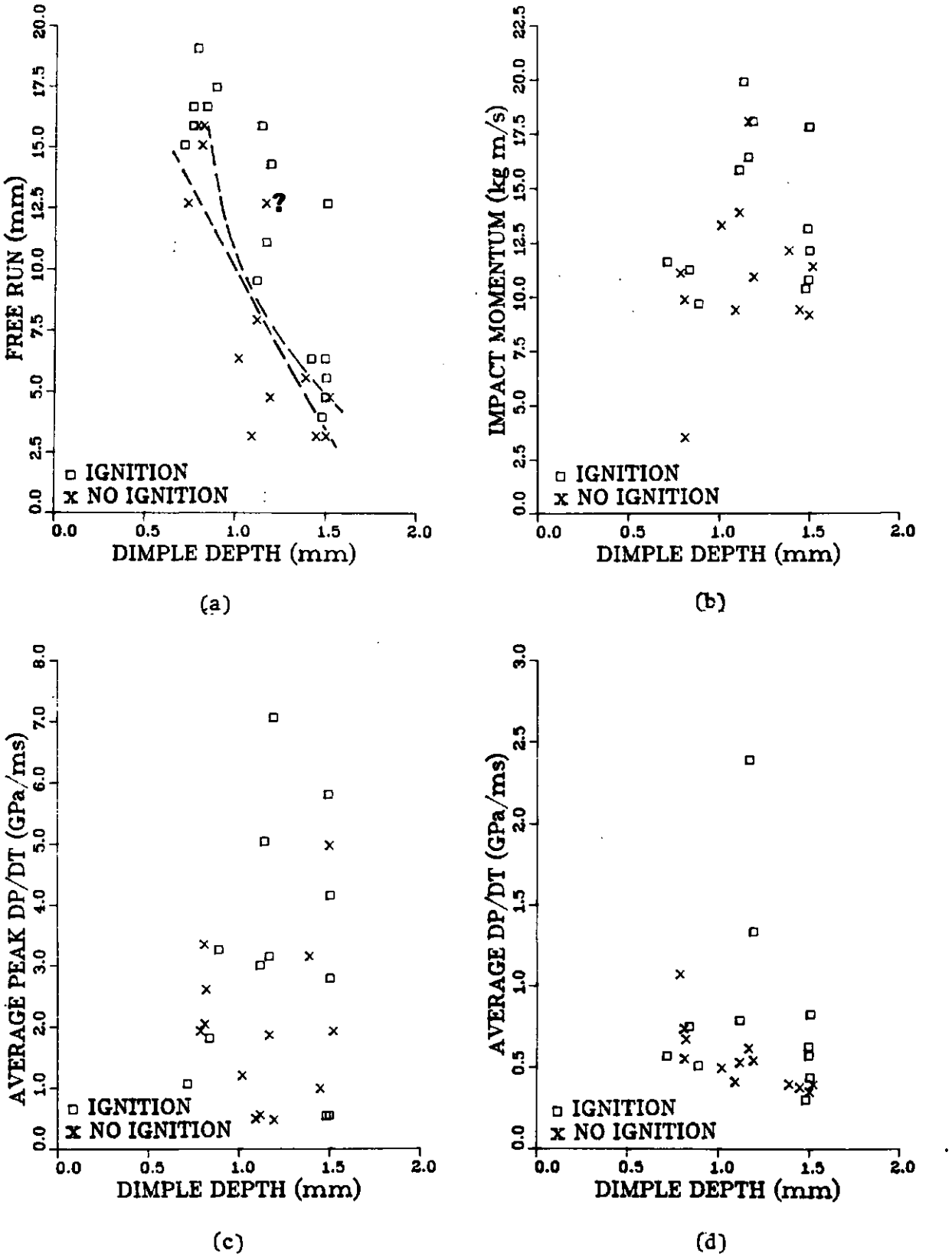

Figure 4. Comparison of Data Segregation Achieved with Each of Four Stimulus Parameters for Sylgard Dimple Tests with 8.5-mm Diameter Dimples.

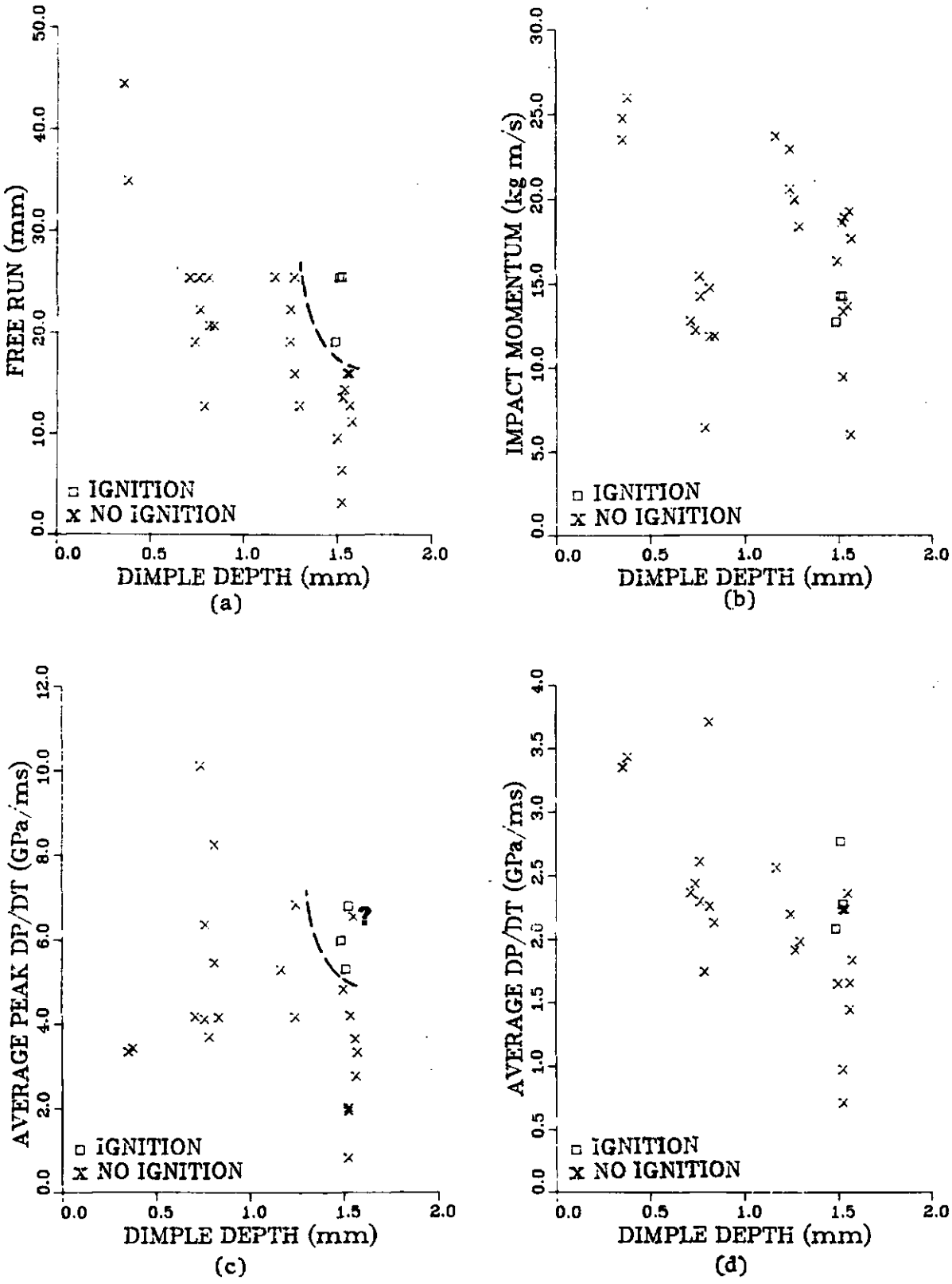

Figure 5. Comparison of Data Segregation Achieved with Each of Four Stimulus Parameters for Vacuum Dimple Tests with 8.5-mm Diameter Dimples.

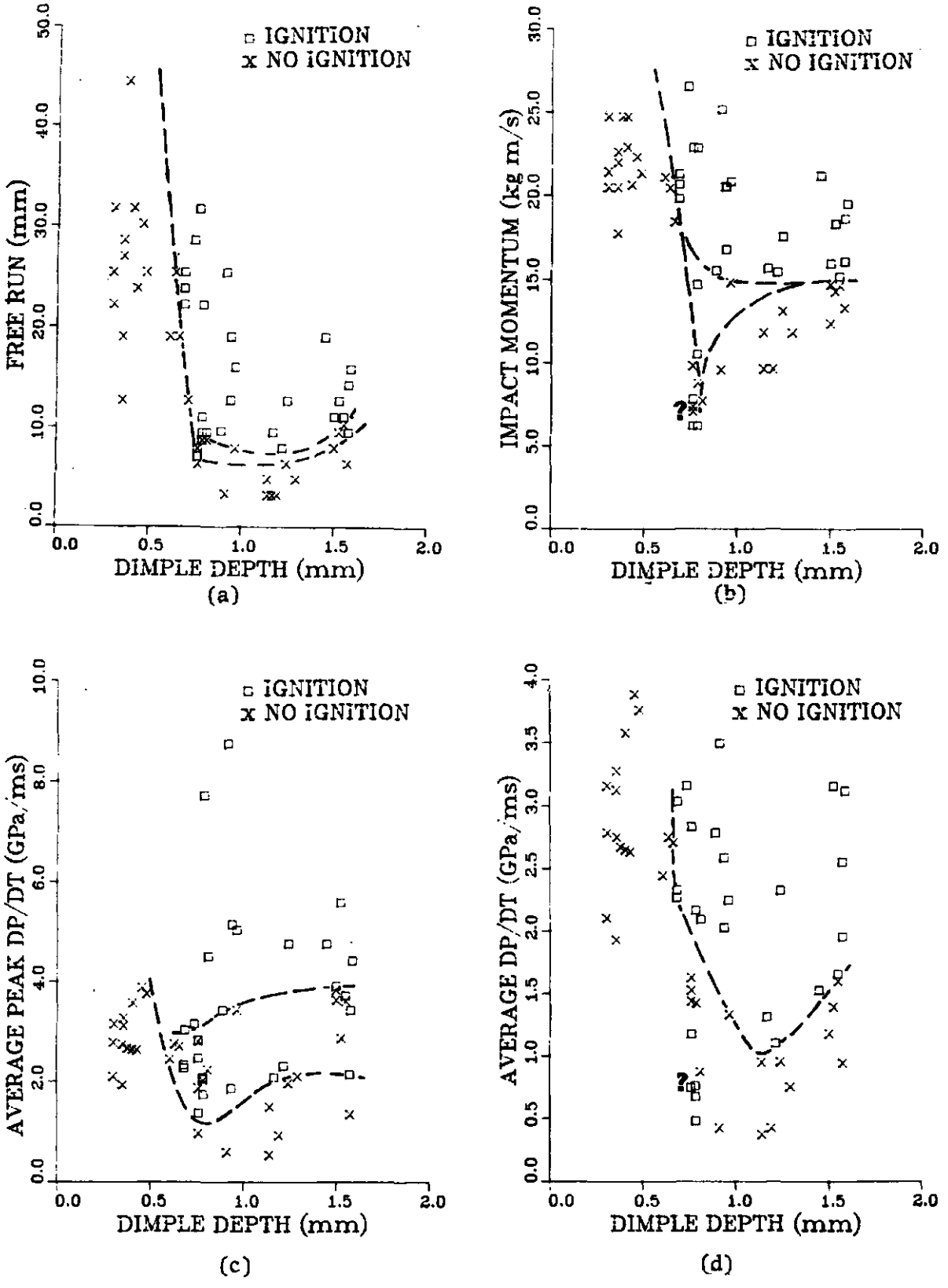

Figure 6. Comparison of Data Segregation Achieved with Each of Four Stimulus Parameters for Dimple Tests with 8.5-mm Diameter Dimples.

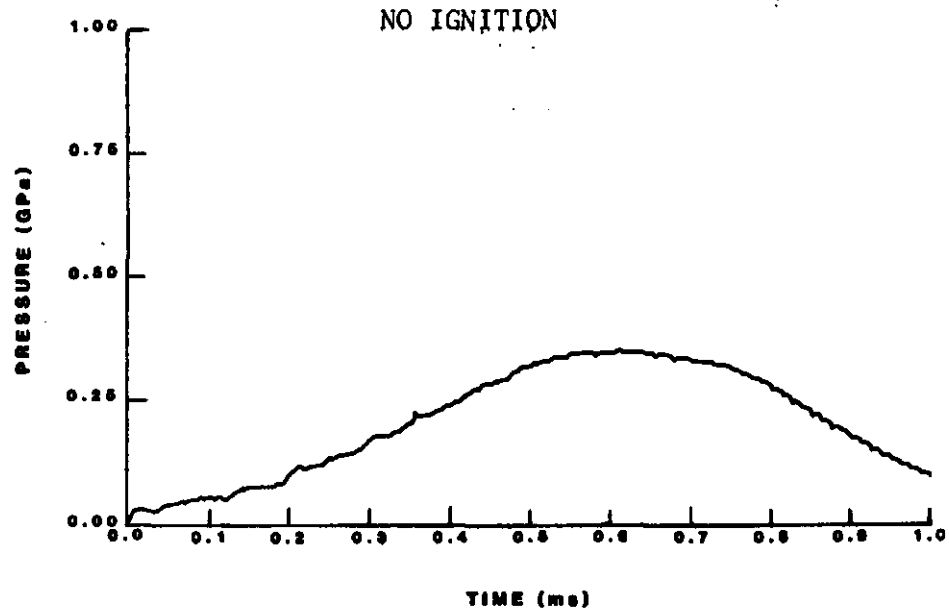

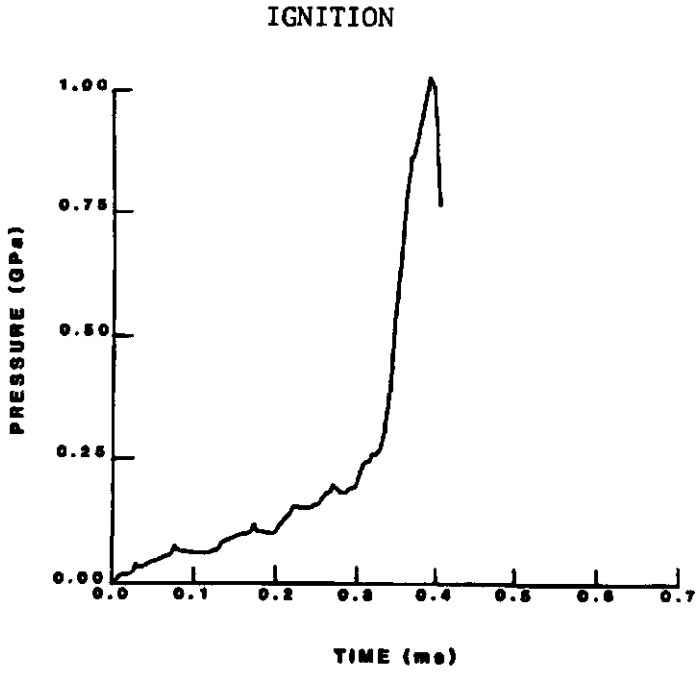

Figure 7a. Typical Manganin Gage Pressure Records for Sylgard Dimple Tests.

NO IGNITION

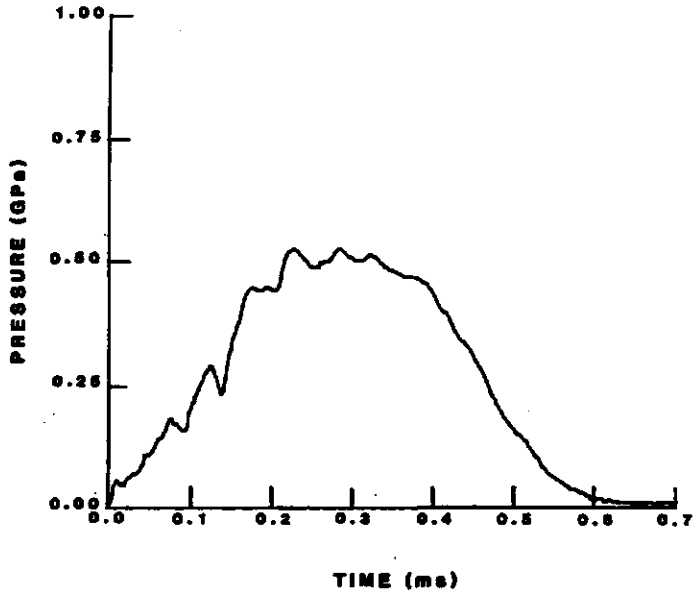

IGNITION

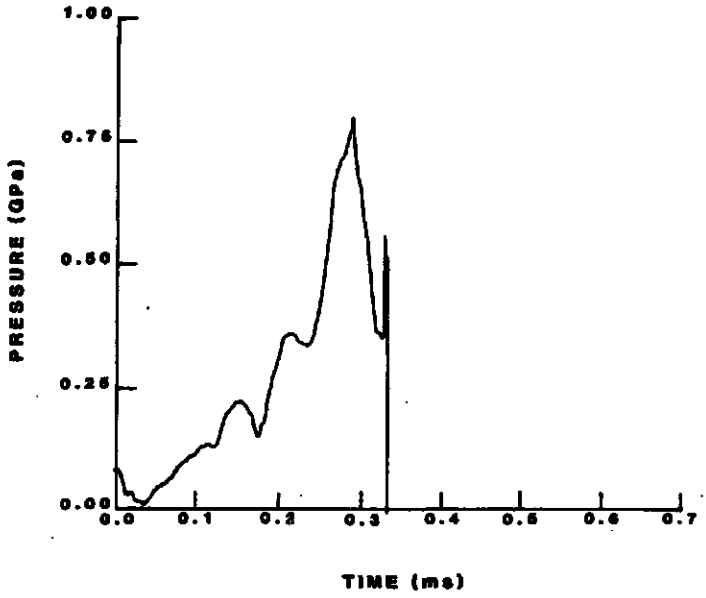

Figure 7b. Typical Manganin Gage Pressure Records for Dimple and Vacuum Dimple Tests.

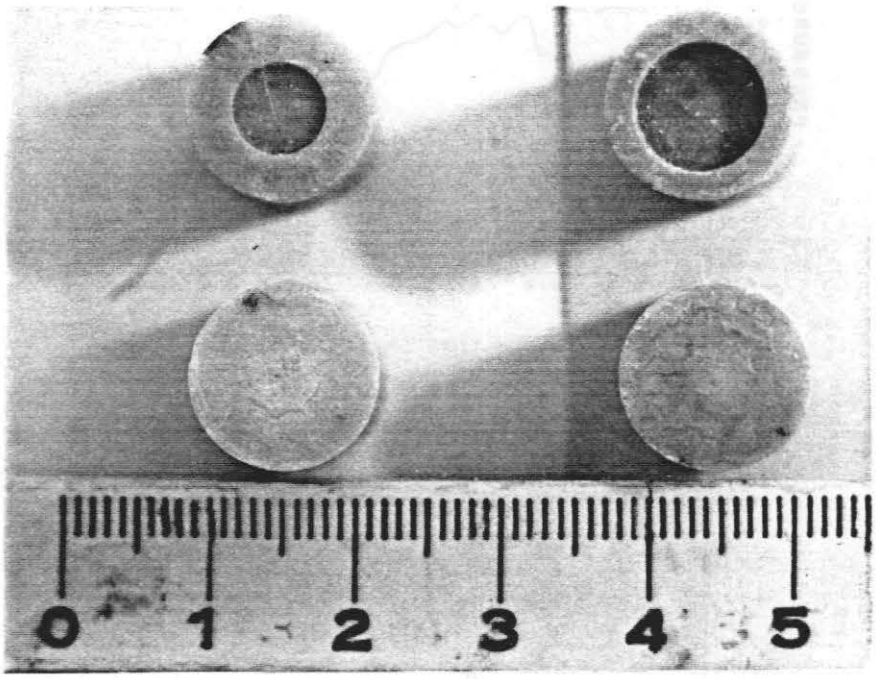

Figure 8. Comparison of Dimpled Samples Before and After Testing.

occur. Between 0.7 and 1.2 mm, sensitivity is independent of dimple depth. The sensitivity then appears to decrease slightly as the dimple depth increases to about 1.5 mm.

Additional observations may be made by comparing thresholds from the three tests as in Figure 9. At the shallow dimple end, the thresholds for air compression only and the combined mechanisms appear to coincide. As dimple depth increases, the sensitivity to the combined mechanisms suddenly becomes independent of dimple depth and is higher than the sensitivity to air compression alone. With a continuing increase in dimple depth, sensitivity to air compression continues to increase while sensitivity to the combined mechanisms decreases slightly such that sensitivity to air compression is greatest. Finally, note that ignition due to deformation alone requires substantially higher stimulus levels.

A number of samples were sectioned in an effort to determine the flow pattern leading to cavity collapse. The sectioned sample shown in Figure 10 exhibits two features of interest. First, the cavity appears to have closed by inward radial flow of material from the shoulders of the dimple. In addition, a conical region of deformation beneath the dimple is visible and the original bottom surface has been displaced upward.

C. Interpretation

The observations suggest that the cavity in the explosive may close in at least two different ways depending on dimple depth. Since the air compression and combined mechanism thresholds coincide with shallow dimples, the collapse of the Sylgard and explosive dimples must be geometrically similar in this case. Cavity closure for shallow dimples presumably occurs by axial flow. The sudden transition observed in the dimple test marks a transition to radial cavity closure, a highly sensitive mode for which dimple depth independence would be expected. The subsequent decrease in sensitivity may be due to a continuing change in the collapse geometry or increasing porosity of the collapsing surface. Since deformation only requires higher stimulus levels we conclude that the primary ignition mechanism in the dimple test is compressive heating of air.

D. Further Observations with Composition B - Effects of Dimple Diameter

Dimple and vacuum dimple tests were subsequently conducted with dimples having a smaller nominal diameter of 6.5 mm and nominal depths of 0.4, 0.8, 1.1 and 1.5 mm. The results for these are plotted in Figures 11 and 12 and the thresholds are compared in Figure 13. Similar results were observed. In this case, no Sylgard dimple tests have been done. Again, ignitions could not be obtained below a cut-off cavity depth for the combined mechanisms. The flat region following the transition is not as long and the decrease in sensitivity with increasing dimple depth is more marked. For the deepest dimples, the ignition thresholds for deformation only and the combined mechanisms appear to coincide. Results with large and small diameter dimples are compared in Figures 14, 15 and 16. In the vacuum case, the 6.5-mm diameter dimples were a little more sensitive than the 8.5-mm diameter dimples as shown in Figure 14. As shown in Figure 15, for the combined mechanisms, the small diameter dimples are generally less sensitive above the cut-off depth. Figure 16 is a plot of free run versus dimple aspect ratio (depth

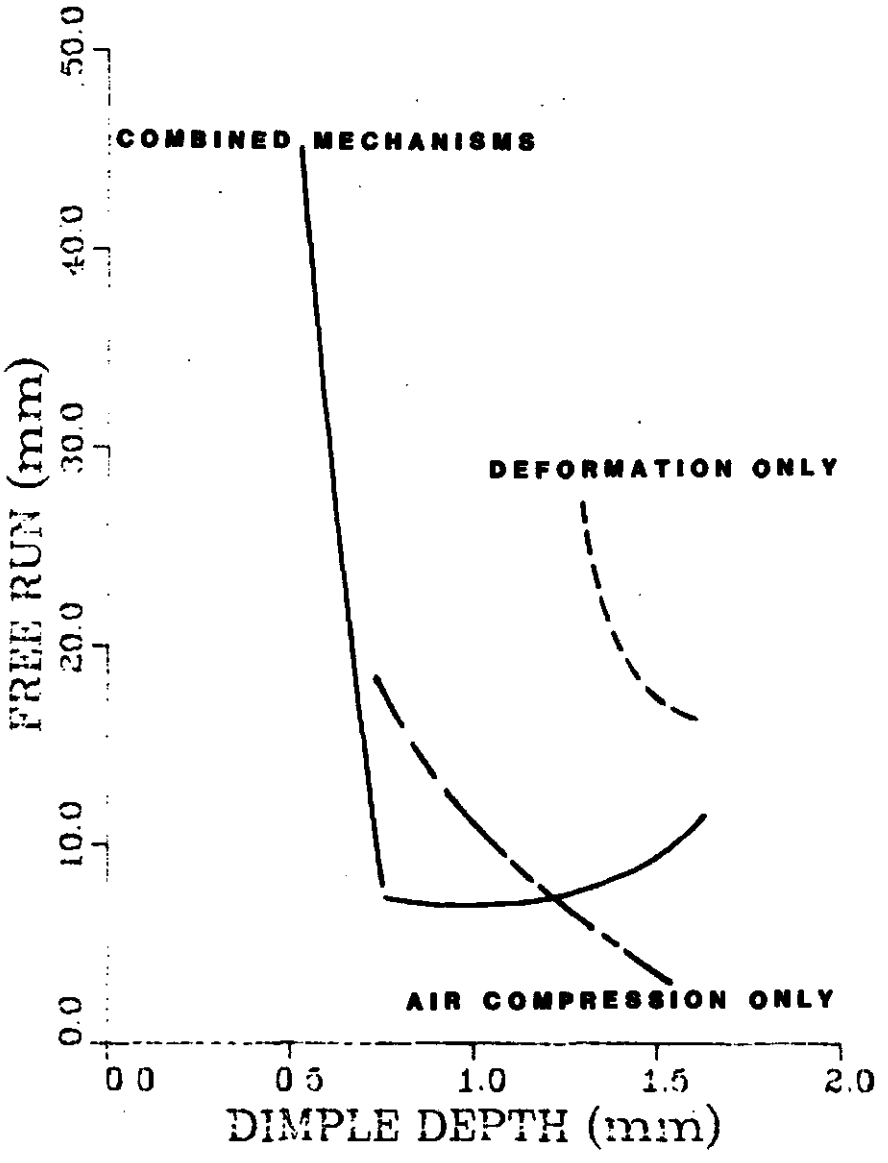

Figure 9. Comparison of Ignition Thresholds for Composition B with 8.5-mm Diameter Dimples.

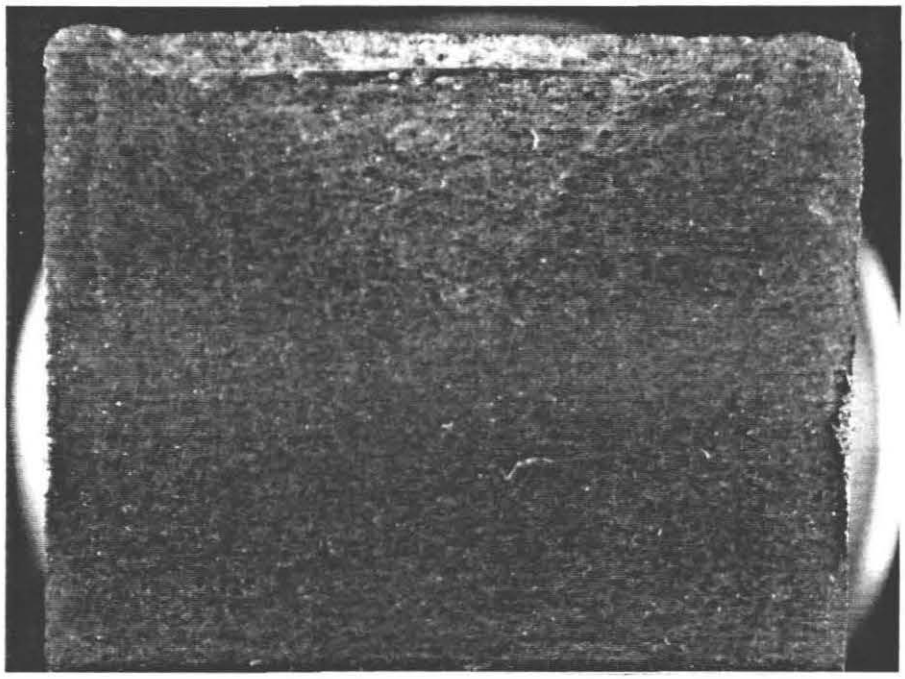

Figure 10. Sectioned Composition B Sample.

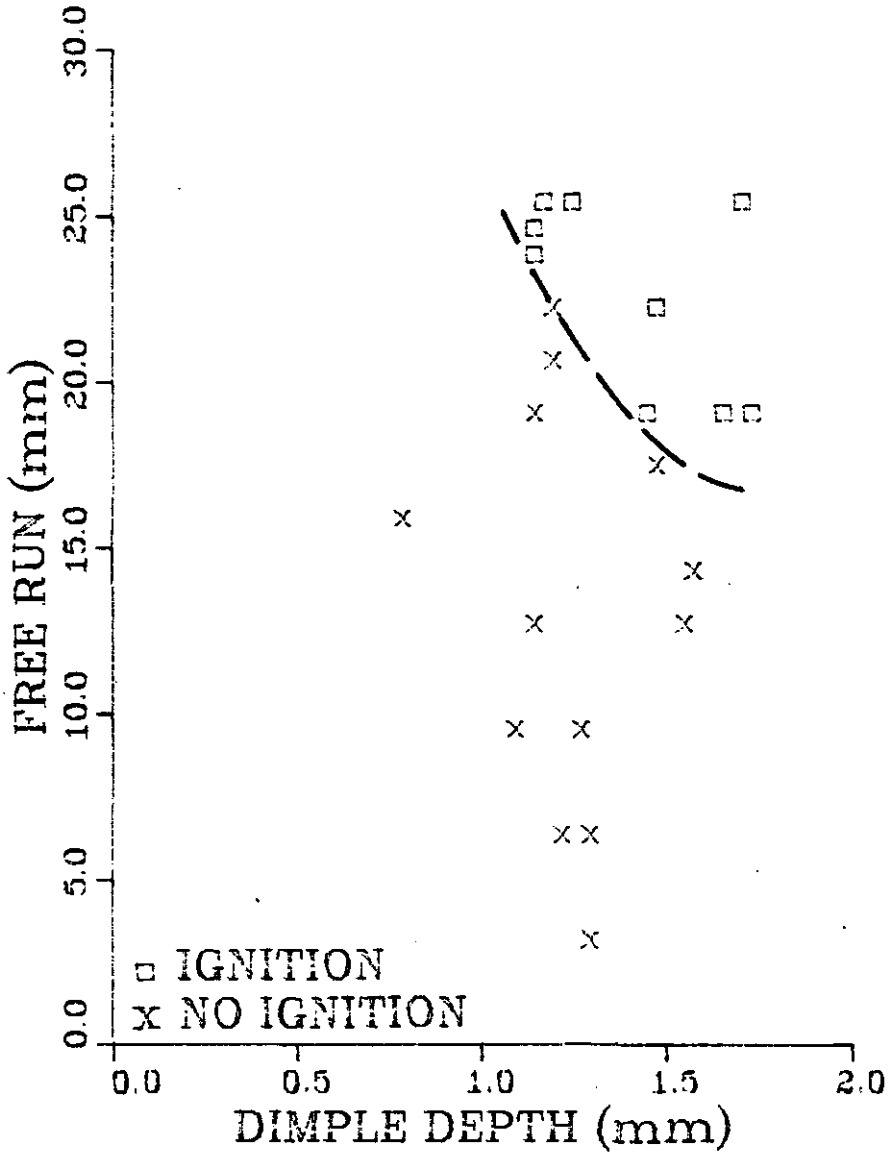

Figure 11. Vacuum Dimple Test Results for Composition B with 6.5-mm Diameter Dimples.

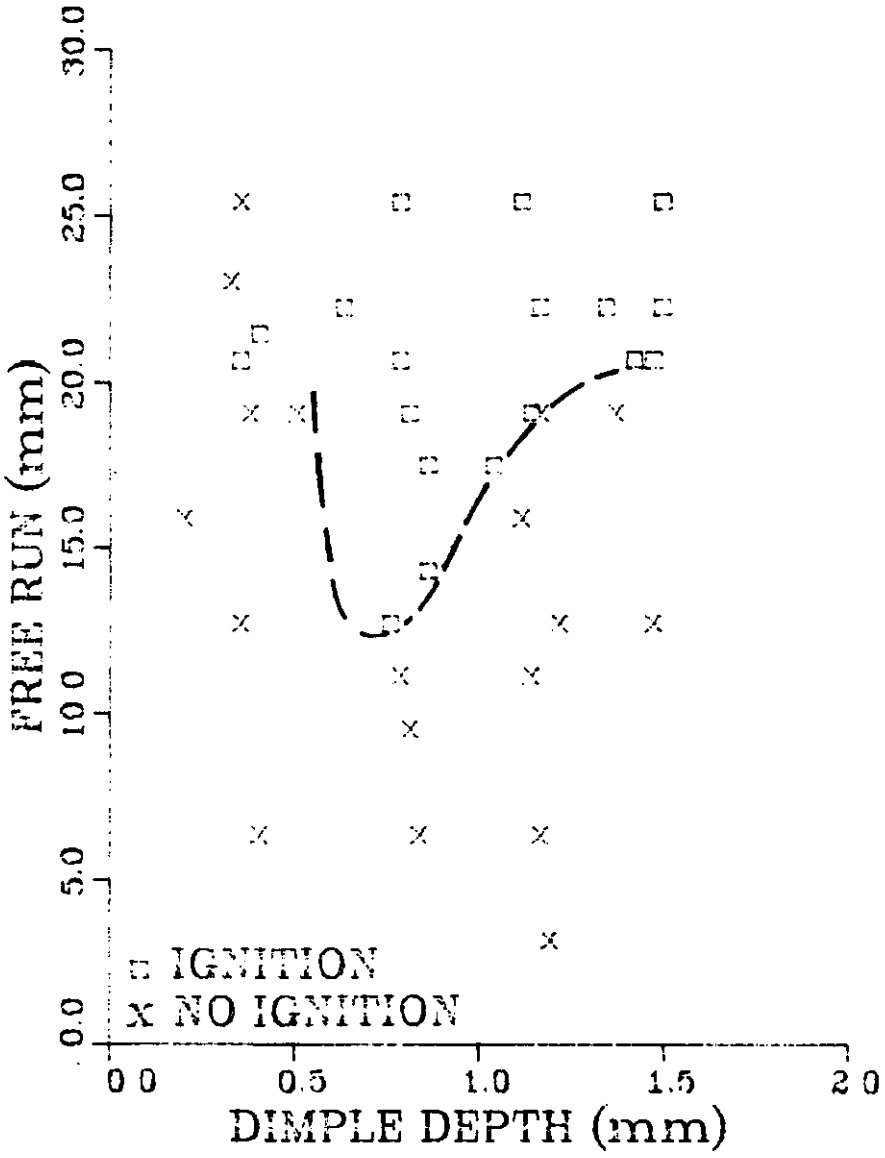

Figure 12. Dimple Test Results for Composition B with 6.5-mm Diameter Dimples

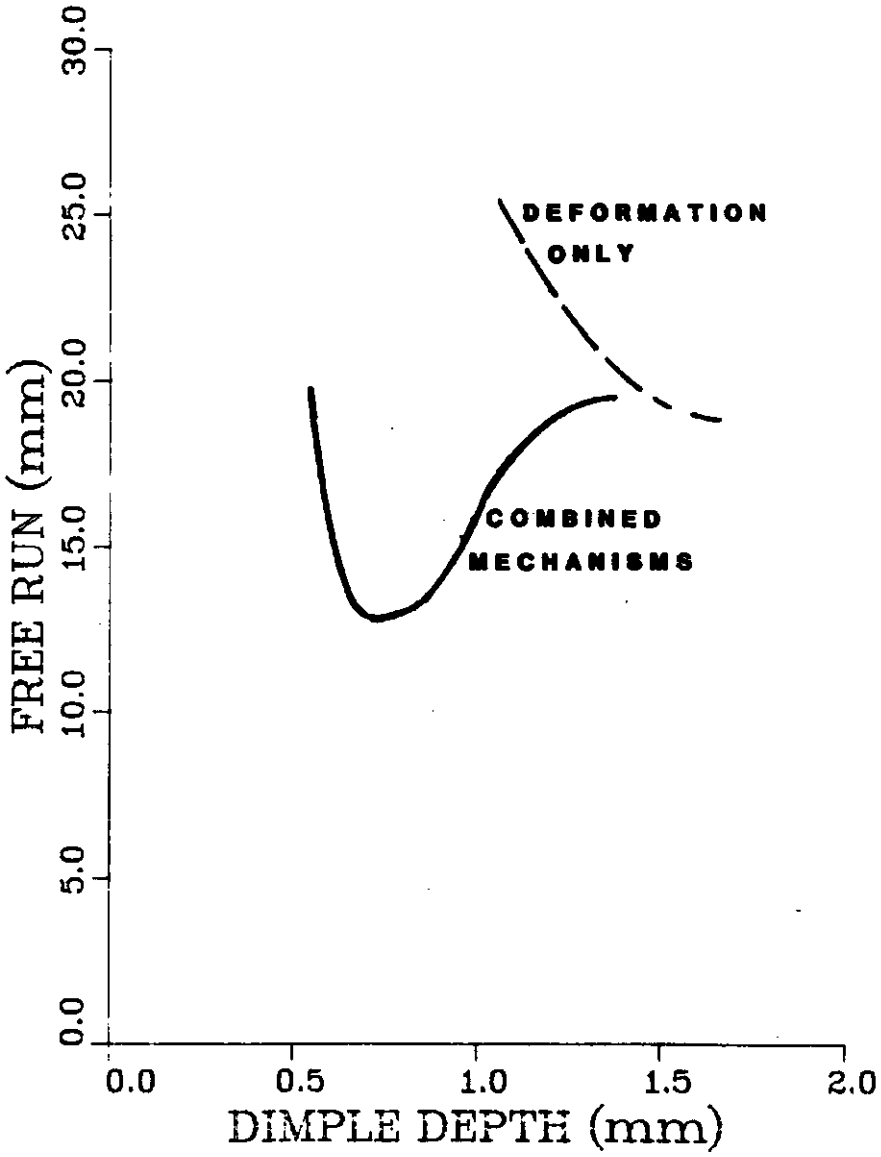

Figure 13. Comparison of Ignition Thresholds for Composition B with 6.5 mm Diameter Dimples.

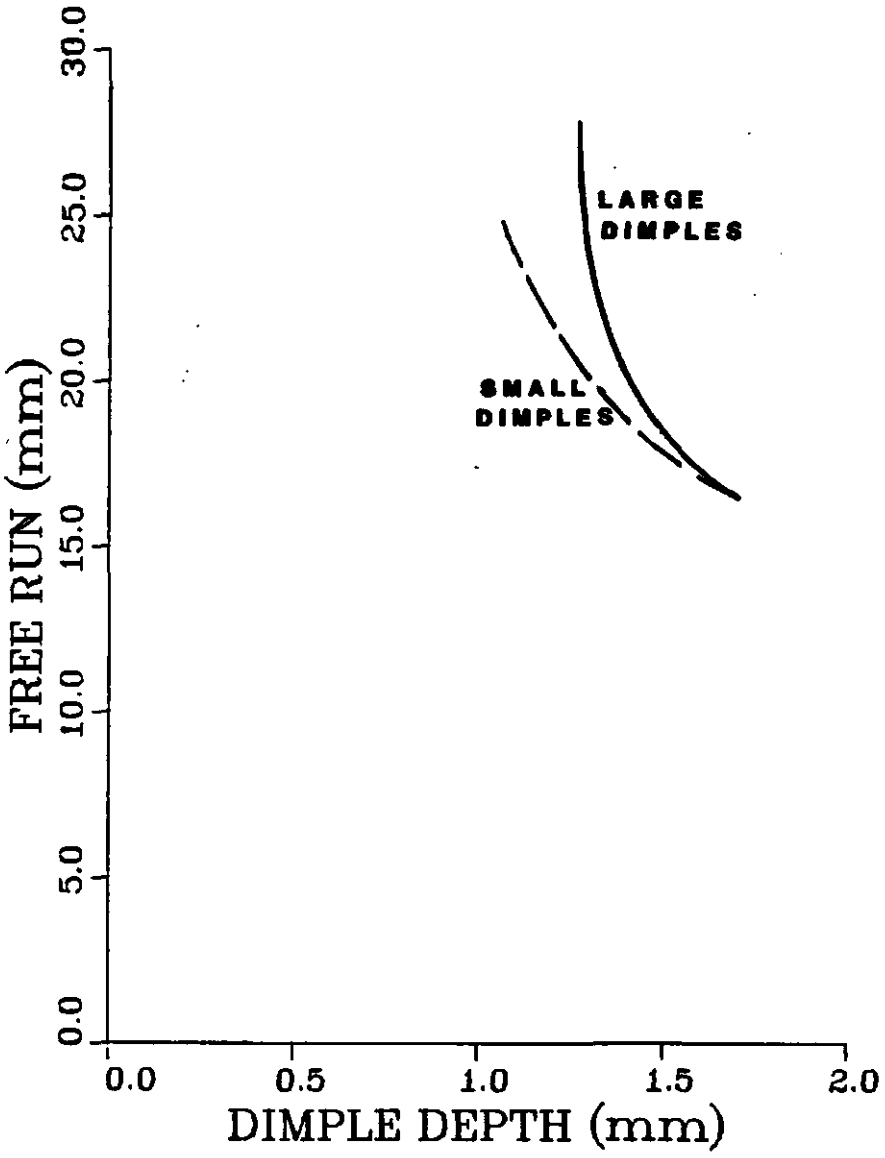

Figure 14 Comparison of 6.5-mm and 8.5-mm Diameter Vacuum Dimple Test Ignition Thresholds.

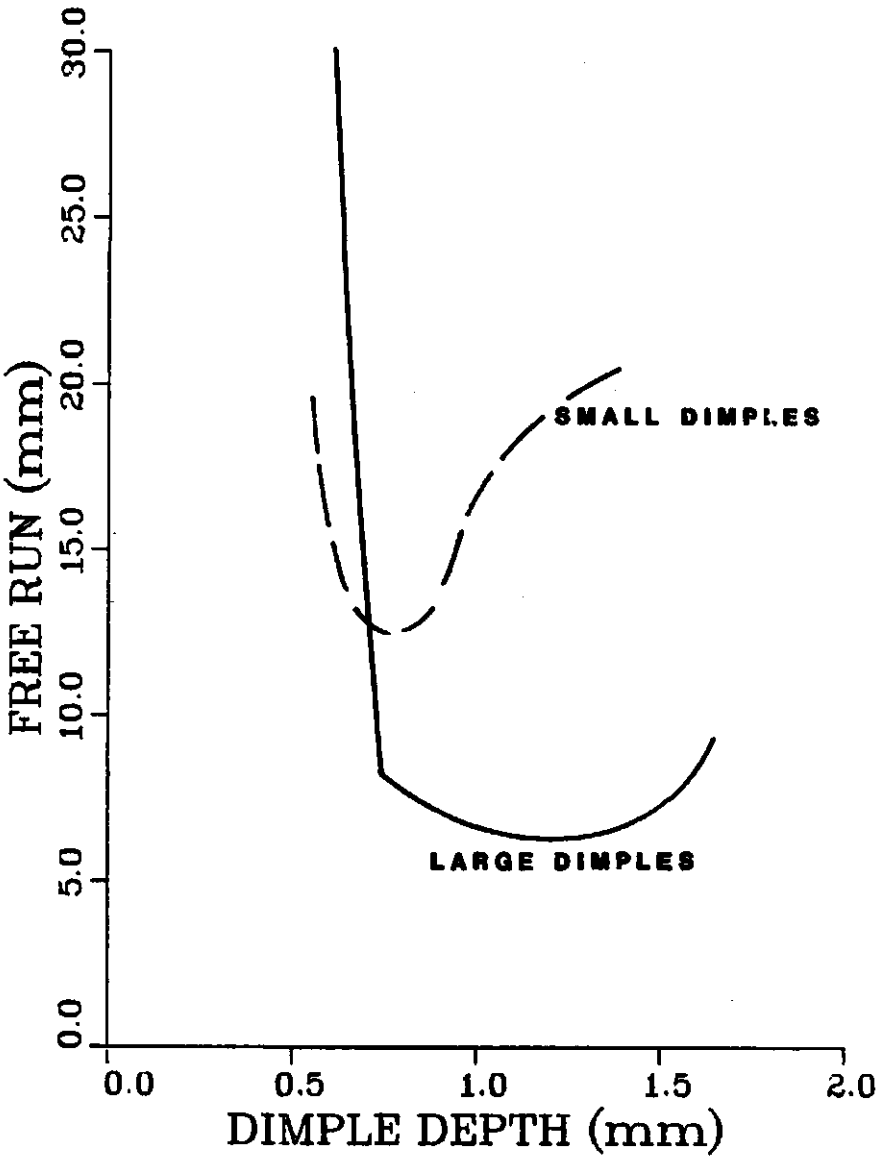

Figure 15. Comparison of 6.5-mm and 8.5-mm Diameter Dimple Test Ignition Thresholds

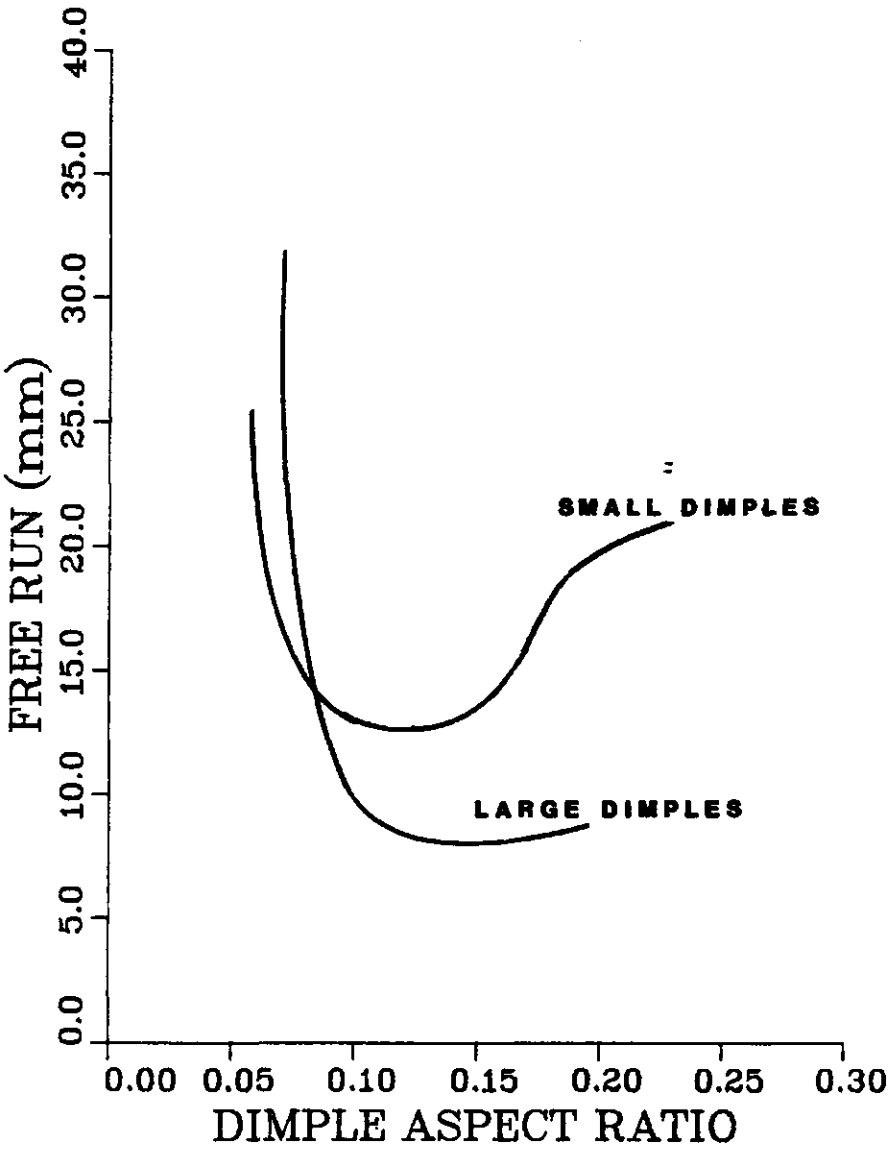

Figure 16. Comparison of 6.5-mm and 8.5-mm Diameter Dimple Test Ignition Thresholds using Aspect Ratio.

divided by diameter). The results show little or no difference in the cut-off aspect ratio for the two diameters. It remains to be determined whether this scaling applies over a wider range of dimple depth and diameter.

V. CONCLUSION

As a result of our work thus far, we have found that when the air compression and deformation heating mechanisms are combined the dominant ignition mechanism is compressive heating of air strongly influenced by the cavity collapse geometry and possibly by alteration of the state of the explosive surface. This result is in agreement with Frey's theoretical assessment,[11] which indicates that the air compression mechanism dominates for large cavities at low pressurization rates. The hypothesis of a transition from axial to radial cavity collapse with increasing dimple depth seems to explain the observed behavior. Deformation heating is the dominant mechanism only for high aspect ratio dimples. The observed cut-off value of dimple depth suggests that it may still be possible to establish a maximum base separation criterion for munitions. However, the way in which this phenomenon depends on dimple geometry remains to be determined. Further, any base separation criterion must be applied to rounds as fired and not as they come off the production line. Thus, a relation between conditions in the field and conditions at production must be established.

REFERENCES

1. J. Starkenberg, "Analytical Models for the Compressive Heating Ignition of High Explosives," Ballistic Research Laboratory Technical Report ARBRL-TR-02225, March 1980, AD# A083889.

2. B. C. Taylor, J. Starkenberg, and L. H. Ervin, "An Experimental Investigation of Composition-B Ignition under Artillery Setback Conditions," Ballistic Research Laboratory Technical Report ARBRL-TR-02276, December 1980, AD# A095348.

3. J. Starkenberg, "Ignition of Solid High Explosives by the Rapid Compression of an Adjacent Gas Layer," Seventh Symposium (International) on Detonation, pp. 3-16, June 1981.

4. J. Starkenberg, L. H. Ervin and D. L. McFadden, "The Ignition of High Explosives in the Launch Environment by Air Compression Heating," BRL Report in press.

5. V. F. DeVost, "Premature Simulator (Final Progress Report)," Naval Ordnance Laboratory Technical Report 74-178, October 1978, AD# B001300L.

6. T. F. Meyers and J. Hershkowitz, "The Effect of Base Gaps on Setback-Shock Sensitivities of Cast Composition B and TNT as Determined by the NSWC Setback-Shock Simulator," Seventh Symposium (International) on Detonation, June 1981.

7. W. O. Soper, "The NSWC Setback Simulator: Stress Environment for Explosive," NSWC TR-84-65, April 1984, AD# B092049L.

8. V. Boyle, personal communication, 1983.

9. J. Hershkowitz, personal communication, October 1979.

10. R. T. Schimmel, "Setback Sensitivity of Composition B Under Conditions Simulating Base Separation in Artillery Projectiles," Picatinny Arsenal Technical Report 3857, 1969, AD# 848944.

11. R. B. Frey, "Cavity Collapse in Energetic Materials," Eighth Symposium (International) on Detonation, July 1985.

This page Left Intentionally Blank

DISTRIBUTION LIST

No. of Copies	Organization
12	Administrator Defense Technical Info Center ATTN: DTIC-DDA Cameron Station Alexandria, VA 22304-6145
1	HQDA DAMA-ART-M Washington, DC 20310
1	Chairman DOD Explosives Safety Board ATTN: Dr. T. Zaker Room 856-C Hoffman Bldg 1 2461 Eisenhower Avenue Alexandria, VA 22331
1	Chairman DOD Explosives Safety Board ATTN: COL O. Westry Room 856-C Hoffman Bldg 1 2461 Eisenhower Avenue Alexandria, VA 22331
1	Commander US Army Material Command ATTN: AMCDRA-ST 5001 Eisenhower Avenue Alexandria, VA 22333-0001
1	Commander Armament R&D Center US Army AMCCOM ATTN: SMCAR-TSS Dover, NJ 07801-5001
1	Commander Armament R&D Center US Army AMCCOM ATTN: SMCAR-LCE, Dr. R. F. Walker Dover, NJ 07801-5001
1	Commander Armament R&D Center US Army AMCCOM ATTN: SMCAR-LCE, Dr. N. Slagg Dover, NJ 07801-5001
1	Commander Armament R&D Center US Army AMCCOM ATTN: SMCAR-LCE B. Fishburn Dover, NJ 07801-5001
1	Commander Armament R&D Center US Army AMCCOM ATTN: SMCAR-LCE W. Voreck Dover NJ 07801-5001
1	Commander Armament R&D Center US Army AMCCOM ATTN: SMCAR-LCE R. Velicky Dover, NJ 07801-5001
1	Commander Armament R&D Center US Army AMCCOM ATTN: SMCAR-LCE P. Marinkas Dover, NJ 07801-5001
1	Commander Armament R&D Center US Army AMCCOM ATTN: SMCAR-LCN, Dr. P. Harris Dover, NJ 07801-5001
1	Commander US Army Armament Munitions and Chemical Command ATTN: SMCAR-ESP-L Rock Island, IL 61299
1	Director Benet Weapons Laboratory US Army AMCCOM ATTN: SMCAR-LCB-TL Watervliet, NY 12189
1	Commander US Army Aviation Research and Development Command ATTN: AMSAV-E 4300 Goodfellow Boulevard St. Louis, MO 63120

DISTRIBUTION LIST

No. of Copies — Organization

1 Director
US Army Air Mobility Research and Development Laboratory
Ames Research Center
Moffett Field, CA 94035

1 Commander
US Army Communications Electronics Command
ATTN: AMSEL-ED
Fort Monmouth, NJ 07703

1 Commander
US Army Communications Electronics Command
ATTN: AMSEL-ATDD
Fort Monmouth, NJ 07703

1 **Commander**
ERADCOM Technical Library
ATTN: DELSD-L (Reports Section)
Fort Monmouth, NJ 07703-5301

1 Commander
MICOM Research, Development and Engineering Center
ATTN: AMSMI-RD
Redstone Arsenal, AL 35898

1 Director
Missile and Space Intelligence Center
ATTN: AIAMS-YDL
Redstone Arsenal, AL 35898-5500

1 Commander
US Army Missile Command
ATTN: AMSME-RK, Dr. R.G. Rhoades
Redstone Arsenal, AL 35898

1 Commander
US Army Tank Automotive Command
ATTN: AMSTA-TSL
Warren, MI 48397-5000

1 Director
US Army TRADOC Systems Analysis Activity
ATTN: ATAA-SL
White Sands Missile Range
NM 88002

No. of Copies — Organization

1 Commandant
US Army Infantry School
ATTN: ATSH-CD-CSO-OR
Fort Benning, GA 31905

1 Commander
US Army Development & Employment Agency
ATTN: MODE-TED-SAB
Fort Lewis, WA 98433

1 Commander
US Army Research Office
ATTN: Chemistry Division
P.O. Box 12211
Research Triangle Park, NC 27709-2211

1 Office of Naval Research
ATTN: Dr. J. Enig, Code 200B
800 N. Quincy Street
Arlington, VA 22217

1 Commander
Naval Sea Systems Command
ATTN: Mr. R. Beauregard, SEA 64E
Washington, DC 20362

1 Commander
Naval Explosive Ordnance Disposal Technology Center
ATTN: Technical Library Code 604
Indian Head, MD 20640

1 Commander
Naval Research Lab
ATTN: Code 6100
Washington, DC 20375

1 Commander
Naval Surface Weapons Center
ATTN: Code G13
Dahlgren, VA 22448

1 Commander
Naval Surface Weapons Center
ATTN: Mr. L. Roslund, R122
Silver Spring, MD 20910

1 Commander
Naval Surface Weapons Center
ATTN: Mr. M. Stosz, R121
Silver Spring, MD 20910

DISTRIBUTION LIST

No. of Copies	Organization
1	Commander Naval Surface Weapons Center ATTN: Code X211, Lib Silver Spring, MD 20910
1	Commander Naval Surface Weapons Center ATTN: E. Zimet, R13 Silver Spring, MD 20910
1	Commander Naval Surface Weapons Center ATTN: R.R. Bernecker, R13 Silver Spring, MD 20910
1	Commander Naval Surface Weapons Center ATTN: J.W. Forbes, R13 Silver Spring, MD 20910
1	Commander Naval Surface Weapons Center ATTN: S.J. Jacobs, R10 Silver Spring, MD 20910
1	Commander Naval Surface Weapons Center ATTN: Dr. C. Dickinson Silver Spring, MD 20910
1	Commander Naval Surface Weapons Center ATTN: J. Short, R12 Silver Spring, MD 20910
1	Commander Naval Weapons Center ATTN: Dr. L. Smith, Code 3205 China Lake, CA 93555
1	Commander Naval Weapons Center ATTN: Dr. A. Amster, Code 385 China Lake, CA 93555
1	Commander Naval Weapons Center ATTN: Dr. R. Reed, Jr., Code 388 China Lake, CA 93555
1	Commander Naval Weapons Center ATTN: Dr. K.J. Graham, Code 3835 China Lake, CA 93555
1	Commander Naval Weapons Station NEDED ATTN: Dr. Louis Rothstein, Code 50 Yorktown, VA 23691
1	Commander Fleet Marine Force, Atlantic ATTN: G-4 (NSAP) Norfolk, VA 23511
1	Commander Air Force Rocket Propulsion Laboratory ATTN: Mr. R. Geisler, Code AFRPL MKPA Edwards AFB, CA 93523
1	AFWL/SUL Kirtland AFB, NM 87117
1	Air Force Armament Laboratory ATTN: AFATL/DLODL Eglin AFB, FL 32542-5000
1	Commander Ballistic Missile Defense Advanced Technology Center ATTN: Dr. David C. Sayles P.O. Box 1500 Huntsville, AL 35807
1	Director Lawrence Livermore National Lab University of California ATTN: Dr. M. Finger P.O. Box 808 Livermore, CA 94550
1	Director Lawrence Livermore National Lab University of California ATTN: Kenneth Scribner P.O. Box 808 Livermore, CA 94550
1	Director Los Alamos National Lab ATTN: John Ramsey P.O. Box 1663 Los Alamos, NM 87545

DISTRIBUTION LIST

No. of Copies	Organization
1	Director Sandia National Lab ATTN: Dr. J. Kennedy Albuquerque, NM 87115

Aberdeen Proving Ground

Dir, USAMSAA
ATTN: AMXSY-D
AMXSY-MP, H. Cohen
Cdr, USATECOM
ATTN: AMSTE-TO-F
Cdr, CRDC, AMCCOM,
ATTN: SMCCR-RSP-A
SMCCR-MU
SMCCR-SPS-IL

No. of Copies	Organization
10	**Central Intelligence Agency Office of Central Reference Dissemination Branch Room GE-47 HQS Washington, D.C. 20502**